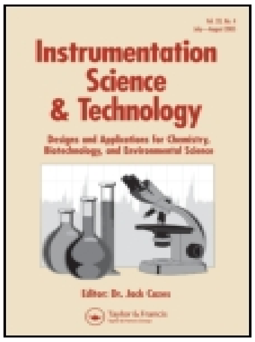

Instrumentation Science & Technology

ISSN: 1073-9149 (Print) 1525-6030 (Online) Journal homepage: https://www.tandfonline.com/loi/list20

DEVELOPMENT AND TESTING OF A NOVEL HIGH-PRECISION STEADY FLOW INSTRUMENT FOR UNSATURATED SOILS

Yong Sang , Longtan Shao & Xiaoxia Guo

Instrumentation Science and Technology, 39:495–509, 2011

ISSN: 1073-9149 print/1525-6030 online
DOI: 10.1080/10739149.2011.623205

DEVELOPMENT AND TESTING OF A NOVEL HIGH-PRECISION STEADY FLOW INSTRUMENT FOR UNSATURATED SOILS

Yong Sang,[1] Longtan Shao,[2] and Xiaoxia Guo[2]

[1]*Key Laboratory for Precision and Non-traditional Machining Technology of Ministry of Education, Dalian University of Technology, Dalian, P. R. China*
[2]*State Key Laboratory of Structural Analysis of Industrial Equipment, Dalian University of Technology, Dalian, P. R. China*

□ *This study is concerned with the development of a novel, high-precision, steady-flow instrument applicable to common unsaturated soils such as clay, silt, sand, gravel soil, and soft soil. The instrument consists of three parts: a high-precision water pressure control system, a high-precision air pressure control system, and a high-precision measurement system. A stepping motor was chosen as the source of water pressure power because it had a high divided driver, reliable operation, simple structure, low cost, and easy maintenance. An electro-pneumatic pressure regulator was used to produce the demanded air pressure. High-precision measurement was archived by a high-resolution grating interferometer, a high-precision balance, and a high-speed 16-bit A/D converter. The device can fully meet the precision requirement of the water pressure, air pressure, and the measurement during the steady flow test for unsaturated soils, which is a very automatic instrument (automatic testing and recording). In this study, volumes of inlet water and outlet water, which are usually difficult to gauge in traditional modes, were gauged by a high-resolution grating interferometer (0.001 mm) and a high-precision balance (0.001 g), and the related experimental study was successfully accomplished.*

Keywords fluid power, steady flow, stepping motor, unsaturated soils, water pressure

INTRODUCTION

The soil–water characteristic curve reflects the relationship between the energy and the amount of water in the soil, which is absolutely necessary to study the water-holding capacity and the moisture movement of the soil. In order to perform these studies, a prototype instrument was

Address correspondence to Longtan Shao, State Key Laboratory of Structural Analysis of Industrial Equipment, Dalian University of Technology, No. 2 Linggong Road, Ganjingzi District, Dalian City, Liaoning Province, 116024, P. R. China. E-mail: shaolt@dlut.edu.cn

developed by measuring water-holding capacity of the soil during a steady flow state.[1] The experimental results indicated that the above apparatus was not always stable and did not have a high-precision measurement and auto saving feature. However, the control system and the measurement methods were recently improved. The latest achievements are introduced in this article.

Getting stable and constant water pressure and air pressure with high precision is the key to success for developing the high-precision steady-flow instrument. The water hydraulic technique using pure tap water as a pressure medium has become a new drive source in comparison with the electric, oil hydraulic, and pneumatic drive systems. High-precision water pressure is not easy to obtain, since water hydraulics have some drawbacks, such as bad lubrication properties, corrosion, cavitation erosion, and low efficiency.[2] On the other hand, the main advantages of using water as the driving media are obvious. In contrast to oil, water is not flammable and is environmentally friendly. These properties make water hydraulics ideal for applications when the fire prevention and environmental protection are the top priorities. At present, only a handful of countries have carried out research and have successfully applied new technology to marine underwater tools and fire-fighting robot systems.[3–7] However, the lack of commercial selection of high-precision water hydraulic components leads to the design and manufacture of this new high-precision steady-flow instrument. With the rapid development of the automation and computer technology, the air pressure control technique as the pneumatic control has enormous impact, because the pneumatic control technology is an important method of industrial automation for its virtues, such as low-cost, high power–weight ratio, non-polluting, simple design, easy to use and maintain, anti-magnetism, anti-explosion, and so on.[8–10] Many pneumatic components had been invented. The electro-pneumatic proportional pressure valve that was invented by SMC Corporation[11,12] converts the electric input signal into an outlet pressure, which in turn controls the pressure in the chamber in real time. The high-precision air pressure is easily obtained by using SMC pressure valves.

In the unsaturated soil testing, the water volume absorbed by the specimen cannot be measured with high-precision with the conventional methods. The water volume changes in the unsaturated soils are different from the specimen volume changes during the triaxial testing, thus they cannot be measured by the digital image processing technique[13,14] or other advanced volume measurement methods.[15] A digital pressure-volume controller as an air volume change indicator was used to measure the air volume changes of the unsaturated soil specimens undergoing isotropic consolidation and axial loading in constant water content tests,[16] but this controller cannot be applied in this instrument directly. A piece of pressure/volume-controlled equipment designed by GDS corporation could measure the water volume change precisely and keep the deviator stress unvaried, and could also measure the volume of water filtrating into the samples exactly,[17,18] but this equipment was relatively expensive. A simple water volume measurement method, which has a high-precision feature with the compensation, has been developed to solve the problems mentioned above in this article.

In this study, a novel, high-precision, steady-flow instrument for the unsaturated soils has been developed. In the past five years, we had already developed two kinds of water pressure controlling devices,[19] which led to a very important role in the new instrument. The first one had been a somewhat like Volume/Pressure Controllers (GDS Instruments Ltd, UK) and Syringe Pumps (Teledyne ISCO, Inc., USA) in some cases, but the device was controlled by a PC, not the embedded computer. The second generating device substituted mechanical structure (crank slider mechanism) for an interpolation-approximation method of the sine wave, and had the ability to modulate amplitude and frequency. The instrument has been developed based on previous work and some problems, such as generating high-precision water/air pressure and achieving high-precision measurement data, have been solved. This instrument has many advantages, such as high-precision measurement, easy control, simple structure, low cost, and no noise. Its unique features are listed here:

1. The volumes of inlet water and outlet water are gauged by a high-resolution grating interferometer (0.001 mm) and a high-precision balance (0.001 g) rather than using the flow meters or other sensors.
2. According to different requirements, water pressure and air pressure can be adjusted continuously and separately.
3. The whole process of steady flow can be recorded continuously and automatically after setting the timer.
4. It is a compacted and integrated instrument of steady flow more than a volume/pressure device.

AN OVERVIEW OF THE NOVEL HIGH-PRECISION STEADY-FLOW INSTRUMENT

The general layout of the novel high-precision steady flow instrument for unsaturated soils is shown in Figure 1. The instrument consists of the standard industrial components and manual parts. The water cylinder is a double-acting pneumatic cylinder (China Fangda Pneumatic Co. Ltd., QGB) with a stroke length of 110 mm and diameter 50 mm. Piston position is measured by the high-resolution grating interferometer (China SF Co. Ltd., GBC-Q-180), which is attached to the nut and has a specified

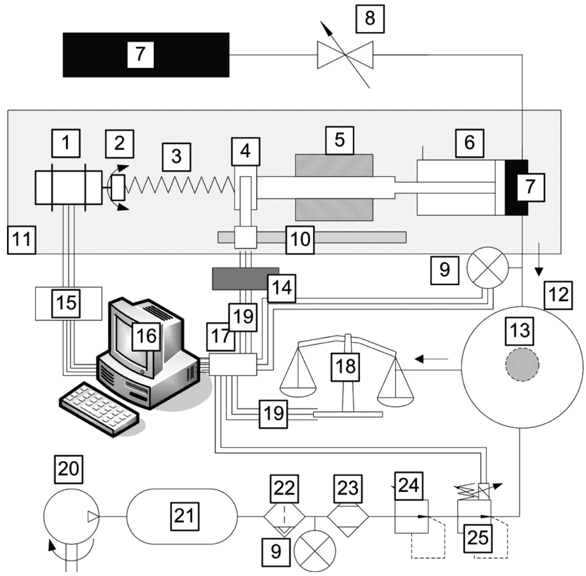

FIGURE 1 Schematic diagram of the laboratory instrument. 1–stepping motor, 2–coupling, 3–ball screw, 4–nut, 5–guide, 6–water cylinder, 7–water, 8–on/off valve, 9–pressure transducer, 10–high-resolution grating interferometer, 11–install bottom, 12–pressure chamber, 13–soil specimen, 14–display meter for the interferometer, 15–driver, 16–PC, 17–hub, 18–high-precision balance, 19–RS232 bus, 20–air compressor, 21–storage tank, 22–filter separator, 23–dryer, 24–manual pressure regulator, 25–SMC E/P regulator.

repeatability of 0.001 mm and a resolution of 0.001 mm for full scale. Stepping motor is used to generate a high-precision water pressure by pushing the water inside the water cylinder, which has a high division of 30000 pulses per revolution. The electronic/pressure regulator (Japan SMC Co., ITV valve) is connected to the pressure chamber. Two pressure transducers are added to measure water pressure and the air pressure. A high-precision balance has a resolution of 0.001 g, which is used to measure the volume of the outlet water. The feedback control algorithms are implemented in a control computer with a PCI data acquisition card. Pressure signals from the field are sent to the control computer via a 16-bit A/D converter. The calculated control signals from the control computer are sent via 12-bit D/A converter to the proportional control valve. Communications are established between the high-resolution grating interferometer, the high-precision balance, and the control computer by using the RS232 interfaces.

It is worth mentioning that the specimen and the high-pressure water are separated by a high air entry ceramic plate. There are many small diameter holes in the ceramic plate, which is roasted with kaolin and is easy for the air to get through. Once the ceramic plate is saturated, the air can not pass through the ceramic plates because of the high capillary water pressure in the holes, so the high-pressure water and the high-pressure air are separated completely. A constant air pressure is applied to the specimen, and as long as the air pressure does not exceed the air entry value of the ceramic plate, the contact cannot be established with the outside water based on the above characteristics of the ceramic plate. The volume of the air in the specimen is constant under a determined air pressure, and there is no relative movement between the air and the soil particles.

WATER PRESSURE CONTROL AND AIR PRESSURE CONTROL

High-Precision Water Pressure Control

The high-precision water pressure control consists of a stepping motor, a motor driver, a water cylinder, a pressure transducer, a ball screw, and the mechanical parts. With the development of the high-speed and high-precision linear motion control systems due to the increasing demand for higher productivity and better product quality in the advanced manufacturing industries, stepping motors are naturally thought to be the most suitable for the applications requiring reliable operation, low cost, simple structure, and easy to use. There is no accumulated error during the rotation. Therefore, stepping motors are usually used as an open-loop control system. The stepping motor driver is the device that changes the pulse signal into the angular displacement, and the accurate speed of stepping motor can be acquired by controlling the pulse frequency. The division technology of the driver can make the real stepping angle become smaller and the maximum division value of the driver in this article is 30000 pulses per revolution. The main advantages of the division are as follows: (1) completely eliminating the low frequency vibration of the stepping motor and (2) raising the output torque and the precision of the stepping motor. The selection principles of the stepping motor are that the maximum torque of the stepping motor is determined by the water pressure, and the maximum speed of the stepping motor is determined by the response demand. The appropriate stepping motor in this article was selected according to the maximum torque and the maximum speed.

As is well known, stepping motors are usually used as an open-loop control system. But in this article, the close-loop control system is realized by measuring the water pressure in real time. The stepping motor used in the water pressure control is a three-phase hybrid stepping motor. Based on the calculated permanence distribution, the equivalent magnetic circuit of the motor can be obtained, and the voltage equation of the three-phase hybrid stepping motor can be derived from a calculation of a flux linkage of each phase based on the equivalent magnetic circuit. The control strategy of the torque can be easily derived from the direct-quadrature axis (d-q) model of the motor. The fuzzy logic controller provides an algorithm, which converts the linguistic control into an automatic control strategy based on expert knowledge. Therefore, the fuzzy logic algorithm is much closer to human thinking in nontraditional logical systems. The task of the fuzzy logic control algorithm is to reach the desired output with no overshoot and reduced settling time. The linguistic control rules are established under the condition of considering the dynamic behavior of the stepping motor, analyzing the error (*E* equals the set water pressure minus the measured water pressure), and its variation (*EC* equals the error from the process output minus the error from the last process output). These control rules are expressed as follows:

$$\begin{cases} \text{If } (E \text{ is NB}) \text{ and } (EC \text{ is NB}) \text{ then } (\text{Pressure is } P_3); \\ \text{If } (E \text{ is PB}) \text{ and } (EC \text{ is PB}) \text{ then } (\text{Pressure is } N_3); \\ \ldots\ldots \end{cases} \tag{1}$$

The properties of the fuzzy logic controller applying to the stepping motor were tested by experimentation. Some experiments (inputting the step signals from 200 kPa to 500 kPa to 200 kPa) had been done that showed that the stepping motor recovered the target pressure without any overshoot. The controlled precision was satisfied and maximum steady error of the water pressure was less than 0.2 kPa. Therefore, the fuzzy logic algorithm presented interesting tracking features. In order to test the insensitivity of the fuzzy controller in response to the external disturbances, some other experiments had been done by abruptly draining the water. The results showed that the controlled system also had a good robustness.

High-Precision Air Pressure Control

The pressure chamber (No. 12 in Figure 1) is filled by the compressed air. This air is first cooled to keep the temperature dependence of the device to a minimum, then, the filtered air passes through an electropneumatic regulator valve (E/P regulator, SMC Corp. of Tokyo, Japan). This valve works on a principle of very fast pressure balancing, which guarantees a stable pressure and quick changes when needed. Given an input signal from 0 to 10 volts, the valve regulates the air pressure for the pressure chamber between 5 and 900 kPa, thus allowing the pressure chamber to take on a continuous variety of configurations. When the input signal decreases, the air pressure is relieved through an exhaust port to allow the corresponding pressure decrease. The valve has a sensitivity within 0.2%

(full span), a linearity within 1% (full span), and a hysteresis within 0.5% (full span), which is satisfied for the steady flow test.

A pressure sensor is mounted in the SMC E/P regulator, which will provide an output pressure feedback to the control circuit. The control circuit will balance the input signal and the output pressure to ensure that the output pressure remains proportional to the input signal. Thus, an additional controller is not needed. Experimental results show that the steady error between the test value of air pressure and the real value of the air pressure always exists. Scattered data 1, scattered data 2, scattered data 3, and scattered data 4 are measured when the manual pressure regulator (No. 24 in Figure 1) is set at 500 kPa, 600 kPa, 700 kPa, and 800 kPa, respectively. The hysteresis of the SMC E/P regulator occurs in response to varying voltages, but it is negligible (within 0.5%). The scattered data are fitting by using the least-squares method. The corresponding polynomials are listed as Equation (2) [the X-axis represents the time (s) and the Y-axis represents the real value (kPa)].

$$\begin{cases} \text{Curve1:}\ \ y = 6\text{E-}10x^4 - 6\text{E-}07x^3 + 0.0002x^2 + 0.9696x - 2.0385 \\ \text{Curve2:}\ \ y = 4\text{E-}10x^4 - 5\text{E-}07x^3 + 0.0002x^2 + 0.9684x - 2.0516 \\ \text{Curve3:}\ \ y = 3\text{E-}10x^4 - 4\text{E-}07x^3 + 0.0002x^2 + 0.9615x - 1.8851 \\ \text{Curve4:}\ \ y = 9\text{E-}11x^4 - 1\text{E-}07x^3 + 5\text{E-}05x^2 + 0.9775x - 2.0052 \end{cases} \tag{2}$$

The steady error between the designed value of the air pressure and the real value of the air pressure is small (less than 1.0 kPa) by fitting methods. In order to test the robustness for the external disturbances, the air pressure changes were recorded during the steady state by abruptly releasing the air. The test results show that the air pressure control system has a high precision with an excellent robustness.

COMPENSATION FOR VOLUME MEASUREMENT

In the unsaturated soil testing, the water volume absorbed by the specimen cannot be measured with high-precision with the conventional methods. The water volume changes for the unsaturated soil are different from the specimen volume changes during triaxial testing, and cannot be measured by the digital image processing technique or other advanced volume measurement methods. A simple water volume measurement method has been developed to solve the above-mentioned problems by using the high-resolution grating interferometer (resolution: 0.001 mm) and a high-precision balance (resolution: 0.001 g) in this article. The inlet water's volume (V_i) and the outlet water's volume (V_o) can be described as:

$$V_i = S_w x_w = \pi R_w^2 x_w, \ V_o = \rho_w m_o \tag{3}$$

where S_w is the cross-sectional area of the water cylinder, x_w is the displacement of the piston, R_w is the diameter of the piston, ρ_w is the density of the water, R_w and ρ_w are the known constants, AND x_w and m_o can be measured by the interferometer and the balance so that V_i and V_o can be calculated.

Large Amount of Air Existing in Cylinder and Pipes

Sometimes the air in the water cylinder or in the pipes is not easy to remove, which will affect the measurement accuracy of the inlet water. Compensation work can not be ignored in this case. As we all know, the difference between the liquid and the gas is that the gas is more compressible. The state of an amount of gas is determined by its pressure, volume, and temperature. The compressibility of the air is analyzed in this article for the air existing in the cylinder and the pipes. The volume change of the air is taken as a reversible multivariable process. In order to set up the mathematic equations, the following assumptions are made:

- The air is ideal.
- The air chamber's thermodynamic states (pressure, temperature, and density) are uniform.
- The air temperature varies slightly from its nominal value.
- The flow leakages are negligible.
- The deformations of the water cylinder, the pressure chamber, and the pipes are negligible.
- The water can not be compressed.

Base on these assumptions, the corresponding equations can be expressed:

$$PV = mRT \Rightarrow V_1 = \frac{m_0 R T_1}{P_1}, \ V_2 = \frac{m_0 R T_2}{P_2} \tag{4}$$

$$\Delta V_t = V_1 - V_2 = m_0 R\left(\frac{T_1}{P_1} - \frac{T_2}{P_2}\right) \tag{5}$$

$$\Rightarrow m_0 \Rightarrow V_1, V_2, V_3 \Rightarrow \ \Delta V_c = V_3 - V_2(V_1) \tag{6}$$

where m_o is the mass of the outlet water; P, P_1, and P_2 are the absolute pressures of the air; V, V_1, V_2, and V_3 are the volume of the air; m is the mass of the air; R is the air constant; T, T_1, and T_2 are the absolute temperatures;

and ΔV_c is the compensation volume. The detailed steps for calculating the compensation volume are introduced as follows:

1. Measuring the volume change ΔV_t using the high-resolution grating interferometer in two different pressures (P_1 and P_2)
2. Calculating the mass of the air, m_0
3. Calculating the real values for the $V_1, V_2, V_3\,(P_3)$
4. Realizing the compensation for the inlet water volume, V_i

Small Air Existing in the Cylinder and Pipes

In most cases, only a small amount of air exists in the water cylinder or in the pipes. The deformations of the water cylinder, pressure chamber, and pipes are not negligible, and the compression of water also needs to be considered. Therefore, Equations (4), (5), and (6) do not apply in this case, and it is difficult to set up the mathematic equation to calculate the volume changes. The only way to measure the volume changes is to obtain them by experiments. For example, we can measure the volume changes when the water pressure is 100 kPa, 150 kPa, 200 kPa, 250 kPa, 300 kPa, 350 kPa, 400 kPa, 450 kPa, 500 kPa, 550 kPa, 600 kPa, 650 kPa, and 700 kPa. Those scattered data will be fitted by using the least-squares method, and the corresponding polynomial can be calculated. Based on the fitting polynomial, the compensation for the volume measurement can be realized when there is only a small amount of air existing in the water cylinder and the pipes.

Leakage Compensation

Leakage can exist in the hydraulic transmission anywhere and anytime. The seals (between the piston and the inner surface of the cylinder), the on-off valves, and the connecters are the major components that cause the leakage. There is no way to make the device into an absolutely leak-free system. The test continues for several hours, and the flow leakage should not be negligible. The mathematic model of the leakage system is not easy to establish. The possible approach presented in this article is to obtain the empirical model through a series of experiments. Experimental results show that the leakage really exists, but it is relatively small (the leakage is less than 2.0 ml within 5000 seconds). The leakages are measured when the water pressure is set at 200 kPa, 300 kPa, 400 kPa, and 500 kPa. The scattered data are fitting by using the least-squares method, and the corresponding polynomials are listed as Equation (7) [the X-axis represents the time (s), and the Y-axis represents the leakage (ml)]. The leakage compensation can be realized by the following polynomials:

$$\begin{cases} 200\,\text{kPa:} \ \ y = -1E\text{-}13x^3 + 7E\text{-}10x^2 + 4E\text{-}06x\text{-}5E\text{-}05 \\ 300\,\text{kPa:} \ \ y = -2E\text{-}14x^3 + 2E\text{-}10x^2 + 4E\text{-}06x - 0.0005 \\ 400\,\text{kPa:} \ \ y = -1E\text{-}14x^3 - 1E\text{-}10x^2 + 5E\text{-}06x + 0.0002 \\ 500\,\text{kPa:} \ \ y = -3E\text{-}14x^3 + 2E\text{-}10x^2 + 5E\text{-}06x + 9E\text{-}05 \end{cases} \tag{7}$$

EXPERIMENTAL

Two sets of experiments were conducted in order to test the novel, high-precision, steady-flow instrument. The first set of experiments was carried out in accordance with the requirements listed in Table 1. Here the first set of tests (No. 1) was introduced. Water pressure, air pressure, the outlet water's volume, and the inlet water's volume were recorded, as Figures 2A and 2B show. The dotted curve shown in Figure 2A was the real water pressure, and the solid curve in Figure 2A was the real air pressure. The solid curve shown in Figure 2B was the real outlet water's volume, and the dotted curve in Figure 2B was the test inlet water's volume. The data in curves in Figure 2B were the initial volume, which should be compensated by considering the impact of the retained air and the leakage. The leakage compensation was realized by Equation (7). As a result, the real water volume data was calculated as the dotted curve shown in Figure 2C shows. In the second set of experiments, we measured the volume changes when the water pressure was 100 kPa, 150 kPa, 200 kPa, 250 kPa, 300 kPa, 350 kPa, 400 kPa, 450 kPa, 500 kPa, 550 kPa, 600 kPa, 650 kPa, and 700 kPa in a relatively short period of time, as Figure 2D shows. Because the time for measuring the volume changes was short, the leakage needs to be ignored in the second experiment. The scattered data in Figure 2D were fitted by

TABLE 1 Requirements of Experiment

No	Water pressure (kPa)	Air pressure (kPa)	Period (min)	Sampling period (s)	Temperature (°C)
1	300	320	>250	1	18
2	350	400	>180	1	18
3	450	500	>150	1	18
4	500	550	>100	1	18
5	550	600	>80	1	18
6	600	650	>60	1	18

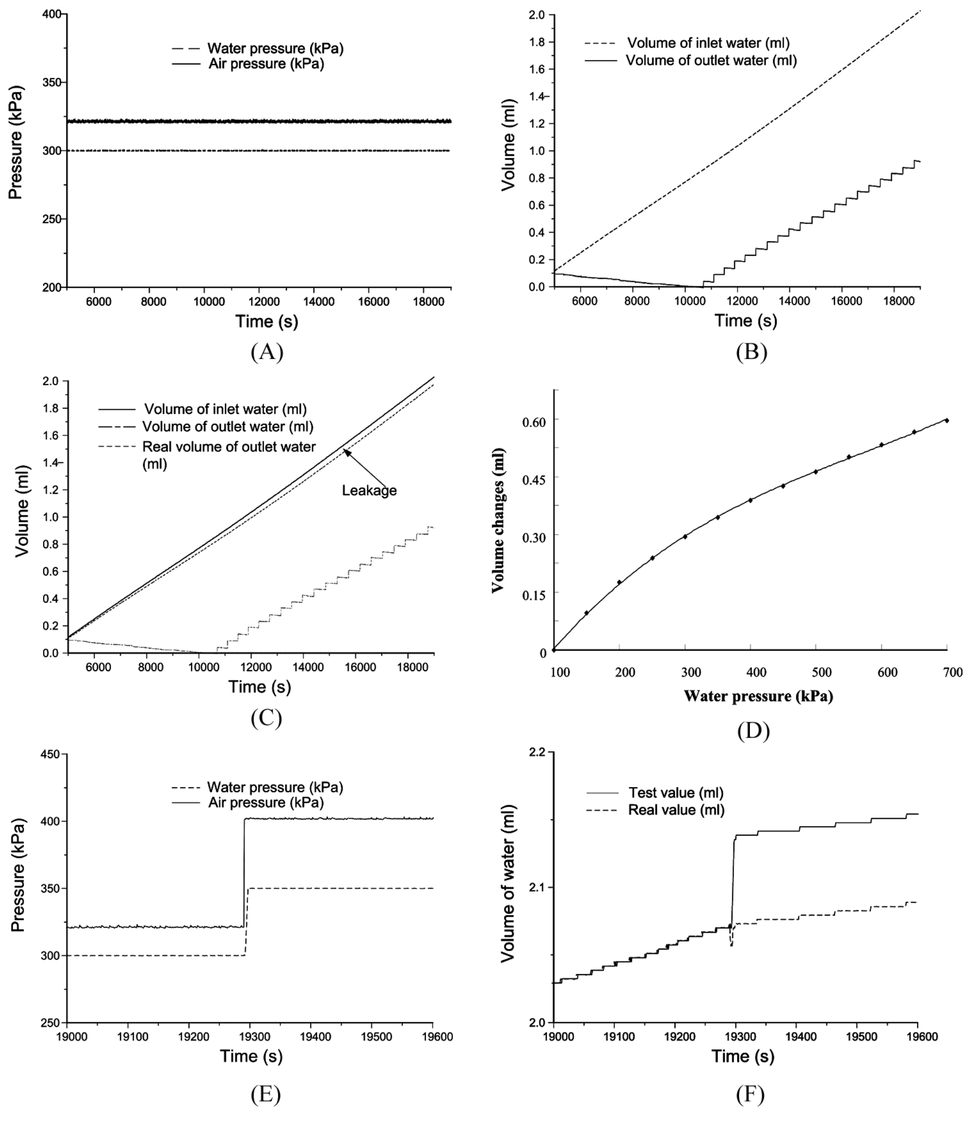

FIGURE 2 Pressure control and the compensation results of the experiments. (A) Pressures of the water and the air; (B) volumes of the inlet water and the outlet water; (C) leakage compensation; (D) relationship between pressure and volume; (E) changes of water pressure and air pressure; (F) air's compensation.

using the least-squares method, and the corresponding polynomials were calculated as Equation (8). Based on the fitting polynomial, the compensation for volume measurement was realized when there was a small amount of air in the water cylinder and the pipes; the compensation result was shown as the dotted curve in Figure 2F. The outcome of the experiment shown in Figure 2 was excellent.

$$300\,\text{kPa:}\ \ y = 2E\text{-}09x^3 - 3E\text{-}06x^2 + 0.0025x - 0.2169 \tag{8}$$

The water-holding capacity and the moisture movement of the soil can be studied based on the above-mentioned testing results. Soil–water characteristics and the unsaturated soil's transmissibility coefficient could be calculated simultaneously. For example, with the increase of matrix suction, water content gradually decreased in the dewatering test. The average matrix suction in the sample can be calculated by the following equation:

$$\left(u_a - \bar{u}_w\right) = u_a - \frac{1}{2}u_w \tag{9}$$

where u_w is the pore water pressure; u_a is the pore air pressure; $\bar{u}_w$ is the average pore water pressure. When the seepage flow of suction in each level is stable, the difference of the increment of high-precision balance's indicator and the reduction volume of water cylinder is the water reduction in the corresponding samples. The dewatering process is completed until the average matrix suction in the sample reaches the predetermined value. Then, the moisture absorption test is performed by reducing the air pressure progressively. The sample absorbs moisture from the outside with the decrease of the matrix suction; the average matrix suction is still calculated by Equation (9). When the seepage flow of suction in each level is stable, the mass difference of outlet water from the cylinder and the mass increment of collected water measured by the high-precision balance are the moisture increment in the corresponding soil sample. The sample is put into the drying oven at the end of the test, so the corresponding water content is determined. Using the changes of water content in each level, the matrix suction in each level is obtained through the inverse calculation. Based on the above methods, the soil–water characteristic curve of silicon powder's dewatering process can be obtained, as Figure 3 shows.

During the above test, it is assumed that the water flows through the soil from top to bottom under the combined effects of the pore water pressure, u_w, and the pore air pressure, u_a. The amount of inflow water and the amount of outflow water in the sample is equal when the suction is stable at each level. The transmissibility coefficient in the dewatering process and the absorbing moisture process can be calculated by measuring the water changes of the water cylinder and water container at a certain period of time. Using Darcy's law, the unsaturated transmissibility

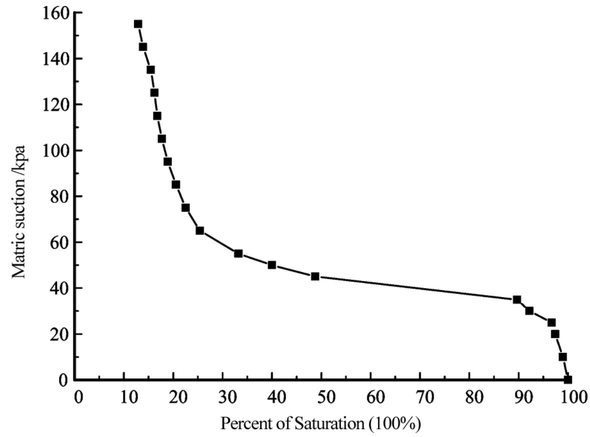

FIGURE 3 Soil–water characteristic curve of silicon powder's dewatering process.

coefficient can be expressed as:

$$K_w = \left(\frac{Q}{A_s t}\right)\frac{L_s}{H_s} \tag{10}$$

where t is the testing time, Q is the flow rate in the testing time, L_s is the thickness of the soil sample, A_s is the area of the soil sample, and H_s is the water pressure difference between the top and the bottom of the soil sample. So the relationships between the transmissibility coefficient of the soil and the matrix suction can be shown in Figure 4.

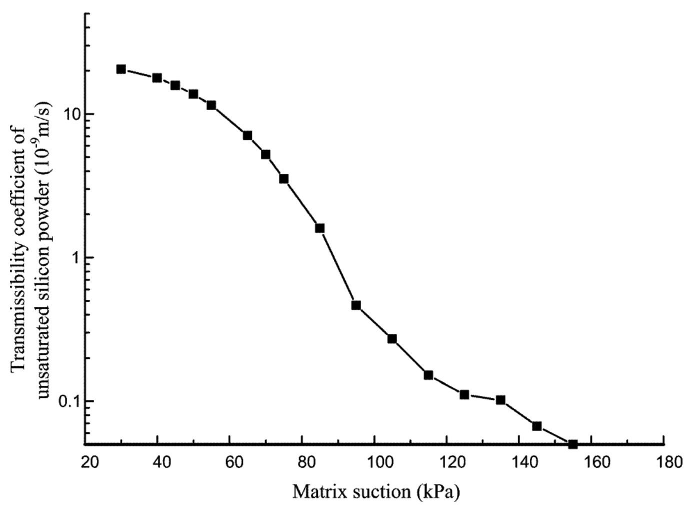

FIGURE 4 Relationships between transmissibility coefficient and matrix suction.

CONCLUSIONS

A novel device called the high-precision, steady-flow instrument was proposed in this article. The instrument consists of three parts: a high-precision water pressure control system, a high-precision air pressure control system, and a high-precision measurement system. These three systems were introduced in detail by the structural and theoretical analytics. The compensation methods for the volume measurement were depicted in this article on the different conditions. A major advantage of the proposed device is that it uses a high-resolution grating interferometer and a high-precision balance so the volumes of inlet water and outlet water can be measured with high precision. A high-speed 16-bit A/D converter, stepping motor, and electro-pneumatic pressure regulator were used to produce the demanded water pressure and the air pressure. Another major advantage of the proposed device is that it is a very automatic instrument because it can test and record the testing data automatically.

The proposed high-precision, steady-flow instrument is believed to be very suitable for use in testing unsaturated soils such as clay, silt, and sand. It will provide a valuable tool for conducting research in the unsaturated soil mechanics field.

ACKNOWLEDGMENTS

We gratefully acknowledge the support by the National Natural Science Foundation of China through grant number 50905022. We would also like to thank the State Key Laboratory of Structural Analysis for Industrial Equipment of China for the time and resources given to this project. Dr. Zhao Honghua has also done some helpful experimental work for this article, and she is gratefully acknowledged by us.

REFERENCES

1. Shao, L.; Liang, A.; Wang, Z.; Sun, J. Manufacture and application of steady seepage equipment for unsaturated soil. *Chin. J. Geotech. Eng*. **2005,** *27*(11), 1338–1340.
2. Rydberg, K.-E. Energy Efficient Water Hydraulic Systems. Fifth International Conference on Fluid Power Transmission and Control, Hangzhou, China, April 3–5, 2001; pp. 11–17.
3. Yoshinada, H.; Yamazaki, T.; Suwa, T.; Naruse, T.; Ueda, H. Seawater hydraulic actuator system for underwater manipulator. *Advanced Robotics*. Fifth International Conference on Robots in Unstructured Environments. 91 ICAR., Pisa, Italy, June 19–22, 1991; pp. 1330–1335.
4. Lane, D. M.; Davies, J. B. C.; Robinson, G.; O'Brien, D. J.; Sneddon, J.; Seaton, E.; Elfstrom, A. The AMADEUS dextrous subsea hand: Design, modeling, and sensor processing. *IEEE J. Oceanic Eng*. **1999**, *24*(1), 96–111.
5. Liljeback, P.; Stavdahl, O.; Beitnes, A. Snakefighter—development of a water hydraulic fire fighting snake robot. 9th International Conference on Control, Automation, Robotics and Vision, Singapore, December 5–8, 2006; pp. 1–6.

6. Muhammad, A.; Esque, S.; Mattila, J.; Tolonen, M.; Nieminen, P.; Linna, O.; Vilenius, M.; Siuko, M.; Palmer, J.; Irving, M. Development of water hydraulic remote handling system for divertor maintenance of ITER. IEEE 22nd Symposium on Fusion Engineering, Albuquerque, New Mexico, June 17–21, 2007; pp. 1–4.
7. Ku, K.; Bradbeer, R. S.; Lam, K.; Yeung, L. F.; Li, R. A novel actuator for underwater robots. *IEEE J. Oceanic Eng.* **2009**, *34*(3), 331–342.
8. Richer, E.; Hurmuzlu, Y. A high performance pneumatic force actuator system: Part I—Nonlinear mathematical model. *J. Dyn. Syst. Meas. Contr.* **2000**, *122*(3), 416–425.
9. Wu, J.; Goldfarb, M.; Barth, E. On the observability of pressure in a pneumatic servo actuator. J. Dyn. Syst. Meas. Contr. 2004, *126*(4), 921–924.
10. Situm, Z.; Pavkovic, D.; Novakovic, B. Servo pneumatic position control using fuzzy PID gain scheduling. *J. Dyn. Syst. Meas. Contr.* **2004**, *126*(2), 376–387.
11. Situm, Z.; Zilic, T.; Essert, M. High speed solenoid valves in pneumatic servo applications. Mediterranean Conference on Control & Automation, Athens, Greece, July 27–29, 2007; pp. 1–6.
12. Wang, X.-S.; Cheng, Y.-H.; Peng, G.-Z. Modeling and self-tuning pressure regulator design for pneumatic-pressure-load systems. *Control Eng. Pract.* **2007**, *15*(9), 1161–1168.
13. Gachet, P.; Geiser, F.; Laloui, L.; Vulliet, L. Automated digital image processing for volume change measurement in triaxial cells. *Geotech. Test. J.* **2007**, *30*(2), 98–103.
14. Rifa'i, A.; Laloui, L.; Vulliet, L. Volume measurement in unsaturated triaxial test using liquid variation and image processing. *Proceedings of the 3rd International Conference on Unsaturated Soils,* Recife, Brazil, March 10–13, 2002; pp. 441–445.
15. Hoyos, L.; Laloui, L.; Vassallo, R. Mechanical testing in unsaturated soils. *Geotech. Geol. Eng.* **2008**, *26*(6), 675–689.
16. Adams, B. A. Air volume change measurement in unsaturated soil testing using a digital pressure-volume controller. *Geotech. Test. J.* **1996**, *19*(1), 12–21.
17. Zhu, Y.; Chen, Z. A. New method of studying collapsibility of loess. *Frontiers of Architecture and Civil Engineering in China* **2009**, *3*(3), 305–311.
18. Laloui, L.; Péron, H.; Geiser, F.; Rifa'i, A.; Vulliet, L. Advances in volume measurement in unsaturated triaxial tests. *Soils and Foundations Journal* **2006**, *46*(3), 341–349.
19. Sang, Y.; Shao, L. The experimental analyses and improvement discussion of a hydraulic sine wave generating device. International Conference on Computer Science and Software Engineering, Wuhan, China, December 12–14, 2008; pp. 132–135.